

MCNP5 SIMULATION OF A LARGE ANGLE X-RAY SCATTERING EXPERIMENT

L. Biddle

AWE

Aldermaston, Reading, Berkshire, United Kingdom, RG7 4PR

lester.biddle@awe.co.uk

ABSTRACT

Scattering of high energy x-rays contributes to the error in object density reconstruction from radiographs of explosively driven hydrodynamics experiments conducted at the Atomic Weapons Establishment. To have confidence in using calculational methods to estimate this scatter the Monte Carlo particle transport code MCNP5 is used to simulate a set of simple static large angle scattering experiments.

A solid stainless steel scattering ball is irradiated with a 6MeV linear accelerator source. Backscattered radiation is measured at five intervals over an ~80 degree range. In this energy regime Compton scattering is the dominant scattering mechanism, modelled in MCNP by the Klein-Nishina relation. The experimental and simulated results are in poor agreement, suggesting there is intrinsic inaccuracy in the way MCNP computes large angle Compton scattering.

This investigation reinforces an earlier study conducted at the Los Alamos National Laboratory (LANL). A near-identical experiment has been conducted at both laboratories, and the two sets of experimental data are in good agreement.

The LANL experiments have been modelled previously in MCNP4B using a different programmatic approach to that employed here. Experimental and calculational results are again found to differ significantly, however the results produced by the two different programmatic approaches are very similar.

This calculational reproducibility with independent programmatic approaches and the reproducibility of the experiment using different facilities suggests MCNP cannot be used to accurately estimate large angle scatter in this regime.

Key Words: MCNP, backscatter

1 INTRODUCTION

The Atomic Weapons Establishment (AWE) is tasked with maintaining the UK nuclear deterrent [1]. In the Comprehensive Test Ban Treaty era this is achieved through a combination of Above Ground Experiments (AGEX) and physics based hydrocode calculations.

As part of the AGEX methodology explosive experiments are conducted in purpose built facilities to underwrite warhead performance. These *Core Punch* experiments investigate the hydrodynamic behaviour of inert weapon simulants.

Core punching uses short pulse (~50ns) flash x-ray machines to perform transmission radiography of a simulant device at time(s) of particular interest during the implosion. The radiographic images are then analysed using a Bayesian statistics based methodology, to obtain

the most probable density distribution for the device at this time(s). Accurate density reconstruction is important in order to validate weapon hydrocodes.

One of the most significant sources of error in density reconstruction from Core Punch data is the presence of x-ray scatter. X-ray scatter is defined as the incoherent background of x-rays that contaminate transmission radiographs in Core Punch experiments. There are various sources of scatter including photons arising from interactions of the x-ray beam with the device, collimation, and components used to protect the detector from the explosive blast.

This scatter comprises two components; forward scatter and backscatter. This is illustrated in Fig. 1, which is a plan view of a typical twin x-ray axis Core Punch experiment as conducted at AWE. Forward scatter consists of primary axis x-rays deflected by small angles, but still reaching the primary detector. Backscatter consists of primary axis x-rays that are scattered through large angles and recorded by the secondary detector.

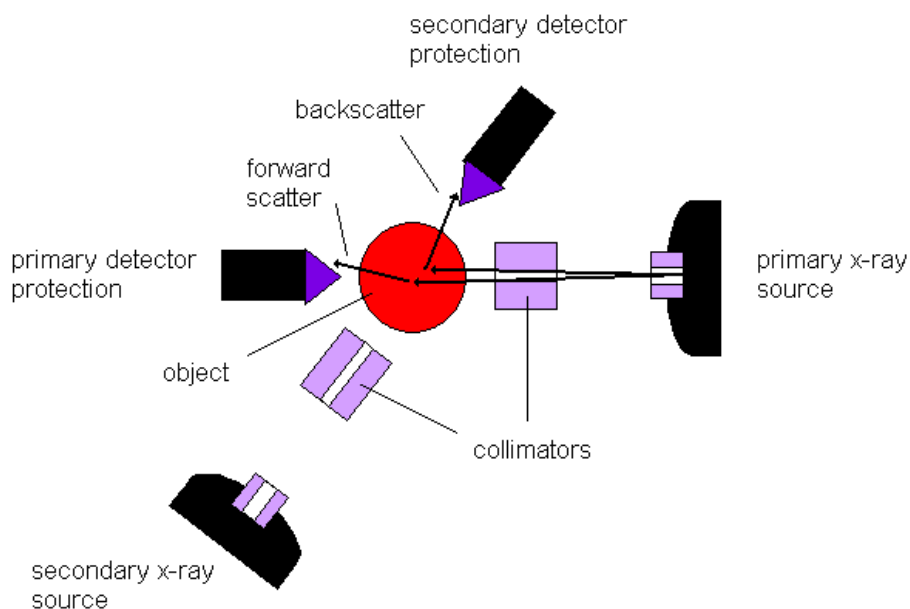


Figure 1. Plan view of a typical Core Punch experiment at AWE

The Monte Carlo N-Particle (MCNP) particle transport code [3] is used at AWE to predict scatter fields in Core Punch experiments. To have a high level of confidence in using MCNP to predict the backscatter in Core Punch trials, the code must be able to accurately simulate a simple static large angle scattering experiment. This paper describes the MCNP simulation of such an experiment.

The purpose of this work was to independently verify earlier near-identical experimental and calculational studies of the capability of MCNP to accurately model backscatter [2].

2 LARGE ANGLE SCATTERING EXPERIMENT

Experiments were performed at AWE using a 6MeV linear accelerator (LINAC) source delivering a dose of 500R at 1m. The general experimental arrangement is shown in Fig. 2. The scattering object used was a 12.7cm diameter solid stainless steel ball.

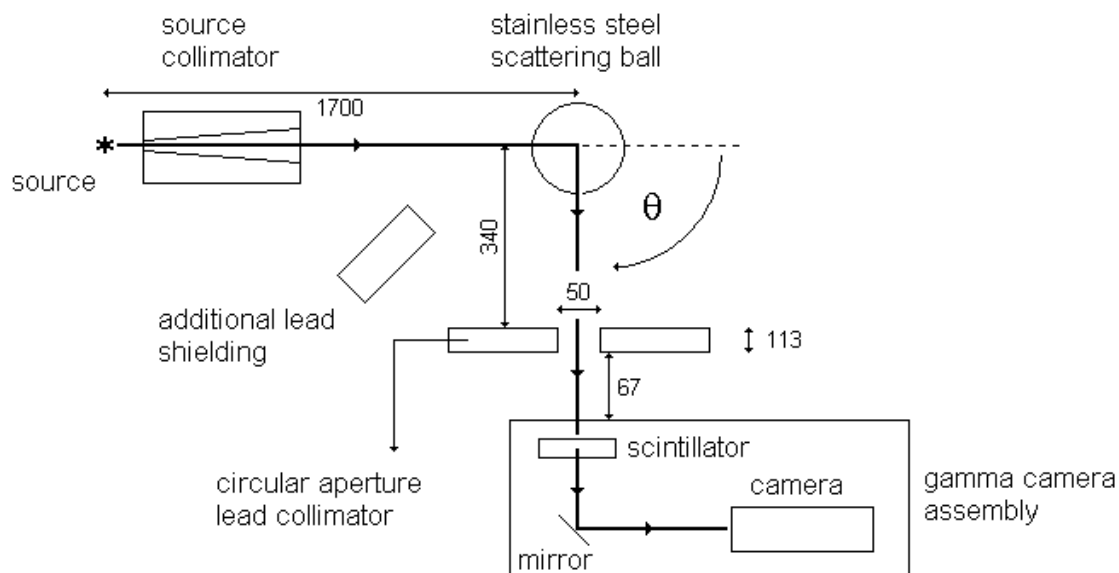


Figure 2. Plan view of experimental geometry to investigate large angle scattering (dimensions are in mm, not to scale)

The detector used was a gamma camera with a CsI scintillator. The gamma camera assembly and lead collimator were positioned at angles of 60, 80, 100, 120 and 142 degrees to the primary axis (θ in Fig. 2).

Additional lead shielding was placed near to the source to reduce any direct dose from the source reaching the detector. For each angle the experiment was conducted both with and without the ball in position in order to quantify the background signal.

This experiment is very similar to a study conducted with the Los Alamos National Laboratory (LANL) Microtron source in 2000, at the same energy [2]. The AWE LINAC and LANL Microtron results are shown in Fig. 3, normalised to the 100 degree results. These are seen to be in good agreement, and show backscatter increasing with angle.

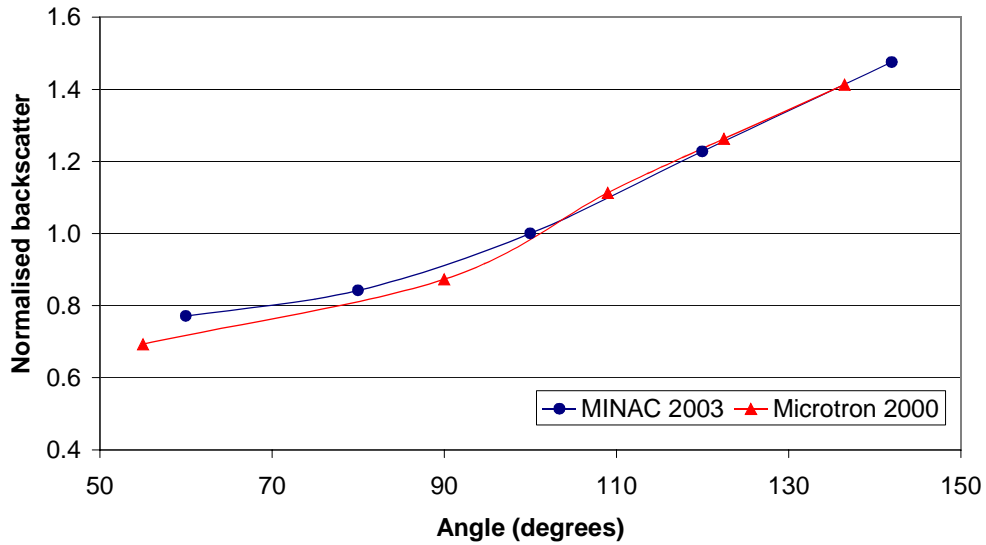


Figure 3. Experimental results taken at the MINAC and the LANL Microtron

3 MONTE CARLO CALCULATIONS

MCNP version 5 has been used to model the experiment conducted at AWE. The chosen methodology divides the problem into two parts; calculating the Bremsstrahlung spectrum produced by the LINAC and determining the level of scatter from the stainless steel ball at the five angles. This approach was used in order to obtain good photon statistics in a reasonably short CPU time.

These two MCNP input files were run in *detailed physics* mode, with both photon and electron transport enabled. Detailed physics mode includes treatment of the binding potential of scattering atomic electrons, and a full treatment of coherent scatter [3].

3.1 Modelling the LINAC X-ray Source

The MCNP simplified source geometry is shown in Fig. 4. A 6MeV 3.28mm diameter parallel beam of electrons is incident on a 1.83mm thick Tungsten target.

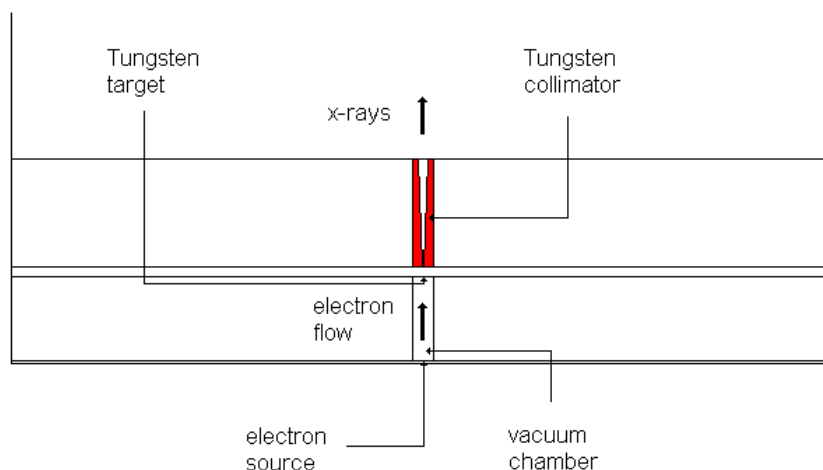


Figure 4. Simplified LINAC source geometry

X-rays produced in the target are detected using a f2 [3] photon flux tally positioned at the back face of the Tungsten source collimator. The resulting Bremsstrahlung spectrum is shown in Fig. 5 normalised to the peak signal, with all the MCNP statistical tests being passed.

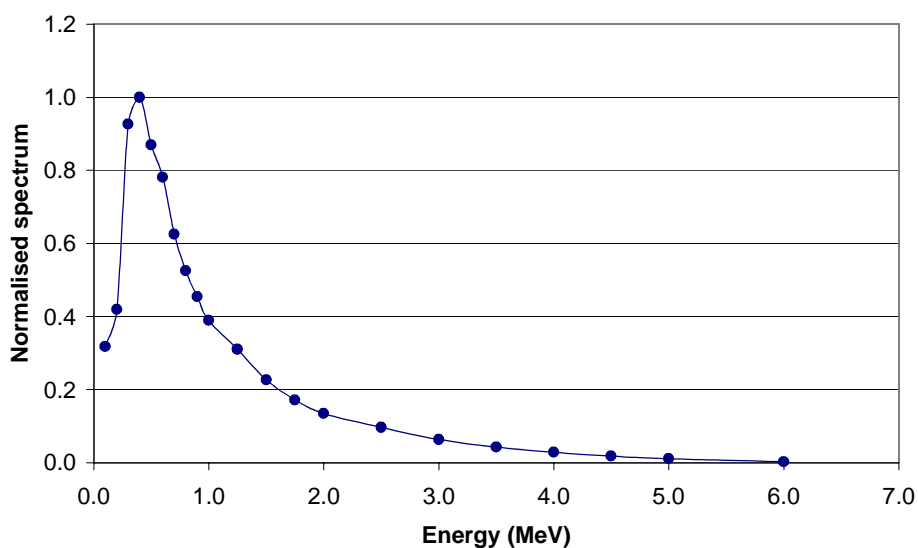


Figure 5. LINAC spectrum

3.2 Modelling the Large Angle Scattering Experiment

The x-ray source spectrum shown in Fig. 5 was used to irradiate a geometry comprising the stainless steel scattering ball, lead collimator and scintillator. A separate calculation was run for each of the five angles, with a translation card (*tr) used to rotate the lead collimator and detector about the centre of the scattering ball.

A f6 energy deposition tally has been used to model the detector. This tally measures the energy deposited in the scintillator volume through photon heating. This approach did not pass all of the MCNP statistical tests; the *pdf slope* test was failed for angles 60, 80 and 100 degrees.

The calculations were thus repeated using a single pixel Flux Image Radiograph (FIR) tally in place of the scintillator and f6 tally. This FIR tally provides an integrated measure of the collided photon flux arriving at the scintillator position, over an area equal to that of the scintillator. In this case all of the relevant MCNP statistical tests were passed. The calculational results, normalised to the 100 degree result, are shown alongside the experimental data in Fig. 6.

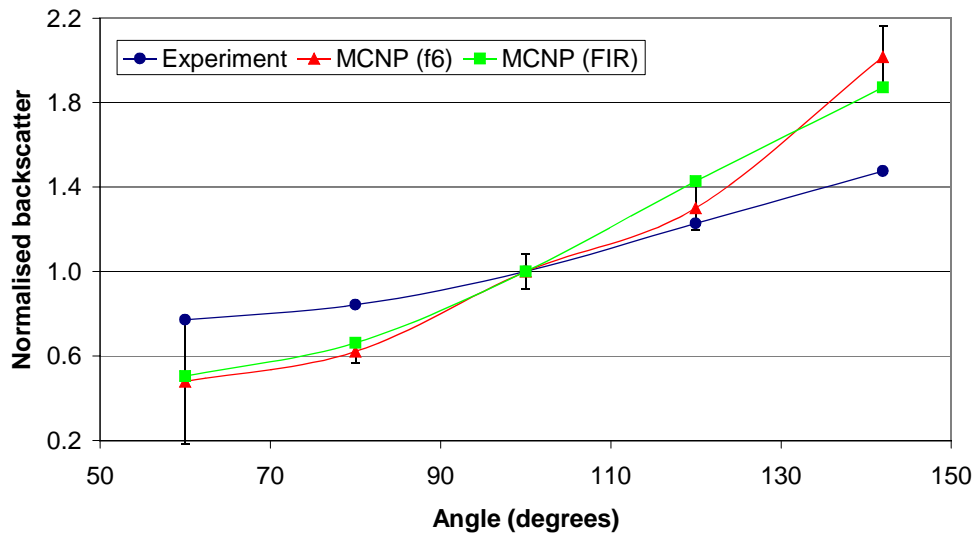


Figure 6. MCNP calculational results

3.3 Discussion

The results of the MCNP calculations follow the same qualitative trend as the experimental data; backscatter increases with angle. The agreement between calculation and experiment is however poor, with the average deviation for the five angles being 21.4% (f6 tally) and 19.8% (FIR tally).

Various factors have been investigated in an attempt to improve the MCNP calculational fit to the experiment, including changing the photon energy cut-off¹. The calculations shown in Fig. 6 used an energy cut-off of 0.09MeV, which is typically used in Core Punch scatter predictions at AWE, and reflects x-ray attenuation by filters and protection materials in the beam.

The only such additional material present in the scattered beam in this experiment is the steel housing of the gamma camera and scintillator assembly. Simple attenuation calculations show this housing to attenuate most photons of energy $\leq 0.09\text{MeV}$.

¹ Threshold below which photons are not transported through the problem

Additional backscatter calculations were conducted with the minimum energy cut-off allowed in MCNP5 (0.001MeV). These results are shown in Fig. 7, and show additional low energy x-rays being detected. The fit to experimental data was not improved.

The calculations have also been repeated with coherent scattering switched off, and with the alloy composition of the stainless steel ball changed. These were investigated as [3] states using a FIR tally in detailed physics mode with coherent scattering switched on is “inadvisable”, and there is inevitably a tolerance on the alloy composition of the stainless steel. Neither of these had a significant effect on the fit to data.

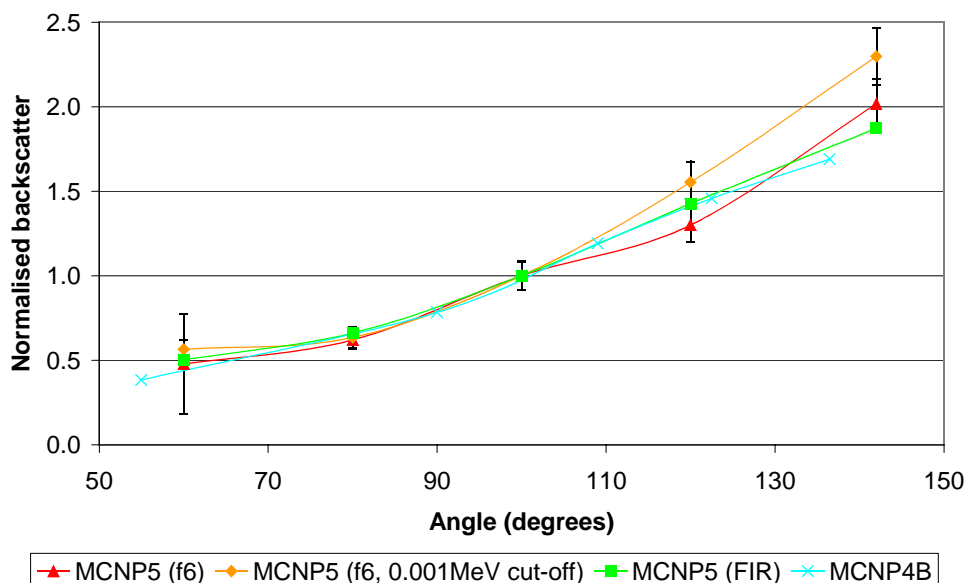


Figure 7. MCNP calculational results

The MCNP results shown in Fig. 6 are shown alongside those obtained in the previous Microtron study [2] in Fig. 7 (MCNP4B trace). The work reported here has been done completely independently from [2], and consequently a different calculational methodology has been used. The two studies have been done with different versions of MCNP, however whilst there have been changes made to the photon and electron treatments between these versions, there appears to be no significant difference in the modelling of this problem.

Fig. 7 shows the two sets of calculational results to be in good agreement. Neither matches its corresponding experimental data. This similarity gives confidence in the MCNP results obtained here for the AWE LINAC experiment, implying that the difference between calculation and experiment could be due to intrinsic inaccuracy in the way MCNP computes large angle scattering in this energy regime. The dominant scattering mechanism in this experiment is Compton scattering, the cross sections for which are calculated in MCNP using the Klein-Nishina equation and the relevant *form factors*². The Klein-Nishina equation is a well documented and tested relation, suggesting that any error would most likely be due to inaccurate form factors, or in the implementation of the Klein-Nishina equation in the code.

² Accounts for electron binding effects in the scattering material

4 CONCLUSIONS

Two independent backscatter studies have been conducted by AWE, both showing significant differences between experimental measurements and MCNP predictions. It is suggested that this disagreement could be due to inaccuracies in the way MCNP computes large angle Compton scattering in the $\sim 0.5\text{MeV}$ regime. Following these studies backscatter continues to be measured experimentally at AWE.

5 ACKNOWLEDGMENTS

The MINAC experiments were conducted by Ian Crotch, Peter Juniper and the author (AWE). Earlier studies at the LANL Microtron were conducted by Steve Quillin, Kevin Parker, John O'Malley and Ian Crotch (AWE).

6 REFERENCES

1. K. R. O'Nions et al, "Science of nuclear warheads" *Nature*, **415**, pp.853-857 (2002).
2. J. O'Malley et al, "Advanced Monte Carlo for Radiation Physics, Particle Transport Simulation and Applications" *Proceedings of the Monte Carlo 2000 Conference*, Lisbon, 23-26 October 2000, pp.357-368 (2001).
3. S. M. Girard (ed.), J. B. Shinn (ed.), *MCNP – A General Monte Carlo N-Particle Transport Code, Version 5*, LA-CP-03-0245 (Los Alamos National Laboratory 2003).